Available online at www.sciencedirect.com
SCIENCE DIRECT
Catalysis Today 113 (2006) 257–262
CATALYSIS TODAY
www.elsevier.com/locate/cattod

Electrochemical nucleation and growth of Co and CoFe alloys on Pt/Si substrates

A. Sahari [a], A. Azizi [a,*], G. Schmerber [b], M. Abes [b], J.P. Bucher [b], A. Dinia [b]

[a] *Laboratoire d'Energétique et d'Electrochimie du Solide, Université de Sétif, Sétif 9000, Algeria*
[b] *Institut de Physique et Chimie des Matériaux de Strasbourg, UMR 7504 du, CNRS-ULP-ECPM, 23 rue du Loess, B.P. 43, 67034 Strasbourg Cedex 2, France*

Available online 4 January 2006

Abstract

Electrochemical nucleation and growth of Co and CoFe alloys on Pt/Si(1 0 0) surface from watts (mixed chloride sulfate) baths were studied by voltammetric, chronoamperometric and AFM measurements. The CoFe alloys were deposited from solution with molar ratio of (1/1) and (10/1). The Scharifker and Hills model was employed to analyse the current transients. For both Co and CoFe (10/1) alloys the nucleation was a good agreement with the instantaneous model followed by 3D diffusion-limited growth. Inversely, for CoFe (1/1) alloy the nucleation was an agreement with the progressive model. It is evident that the compositions of the electrolyte influence greatly the type of nucleation. The atomic force microscopy (AFM) images revealed a compact and a granular structure of the electrodeposited Co layers and CoFe alloys.

PACS: 81.15 Pp; 68.55 s; 81.10.Aj; 75.50

Keywords: Cobalt; CoFe; Electrodeposition; Nucleation; Electrochemical growth; Morphology

1. Introduction

Electrochemical deposition of metals and alloys onto metallic substrates plays an important role in many modern technologies. It is a very attractive method due to its easy application and low cost, in comparison with other deposition techniques. Co and its alloys are eligible materials for application in opto-electronic and magnetic devices [1–4]. Electrochemical Co film growth on various substrates and experimental conditions has been widely studied [5–11]. A progressive nucleation mode was established in chloride baths, for the electrocrystallization of Co on carbon and gold substrates [5,6]. During early stage of Co elctrodepsition, it is established that deposition depends generally on pHs solution [7,8]. In fact, at pH 9.5 a transition from 2D instantaneous to 3D progressive nucleation mechanism was observed. At pH 4.5 the nucleation mechanism is 3D progressive. In sulfate solution, pH 6, that Co deposition consistent with the progressive nucleation model followed by 3D diffusion-limited growth [9]. However, in mixed chloride sulfate solution a transition from progressive to instantaneous nucleation mechanism was established for Co deposition on Pt and Au(1 1 1) substrates at pH 4.2 and [10,11]. Also, various works on the electrodeposition of CoFe alloys in different electrolytes have been carried out [12–16]. In particular, the growth, morphology and microstructure properties of alloys obtained depend on electrodeposition conditions: pH solution, applied potentials and electrolyte composition. A similar behaviour to that of pure Co was found in sulfate and chloride electrolytes [17,18]. However, very little is known about how growth electrodeposited CoFe alloys in mixed chloride sulfate bath, and its mechanism of nucleation and growth. One of great difficulties found in study of nucleation mechanism in early stage of growth in this type of materials is associate to co-deposition phenomena. It is known, electrodeposition of binary alloys of the iron group metals (Co, Ni and Fe) exhibits the phenomenon known as anomalous co-deposition [19]. In the anomalous co-deposition, the less noble metal deposits preferentially; consequently, its relative content in the alloy deposit is much higher

* Corresponding author. Tel.: +213 36 92 51 33; fax: +213 36 92 51 33.
E-mail address: aziziamor@yahoo.fr (A. Azizi).

0920-5861/$ – see front matter © 2005 Elsevier B.V. All rights reserved.
doi:10.1016/j.cattod.2005.11.075

than in the solution. These types of alloys can be also controlled via electrochemically parameters and its mechanism of nucleation may be well known.

In this work, we present experimental results of electrochemical nucleation and growth of Co and CoFe alloys on a Pt/Si(1 0 0) substrate in mixed chloride sulfate baths.

2. Experimental

Cobalt layers and CoFe alloys were electrodeposited on thick platinum films evaporated on Si(1 0 0) substrates. From a Si(1 0 0) wafer 1.5 cm × 2 cm, pieces were cut and used as substrates. The piece was cleaned in a 5% HF solution and then immediately transferred to the evaporated room. After the cleaning procedure, about a 50 nm thick Pt layer was evaporated by molecular-beam epitaxy (MBE) onto each Si piece at low temperature (77 K). The area of working electrode is about 0.50 cm × 0.6 cm and is transferred in the electrochemical cell. The auxiliary electrode was a platinum electrode. A sutured calomel electrode (SCE) was used as reference electrode, and was connected to the main cell through a lugging capillary. The electrolyte for electrochemical deposition of Co alone consists of 100 mM $CoSO_4$, 10 mM $CoCl_2$ and 1 M Na_2SO_4 solutions containing 500 mM H_3BO_3 (pH ≈ 3.8–4 adjusted by sulphuric acid). CoFe alloys were deposited from 100 mM $CoSO_4$ + 10 mM $CoCl_2$ + 100 mM $FeSO_4$ (ratio 1/1), 100 mM $CoSO_4$ + 10 mM $CoCl_2$ + 10 mM $FeSO_4$ (ratio 10/1), in 1 M Na_2SO_4 and 500 mM H_3BO_3 solutions. The electrolyte composition was chosen in order to control hydrogen evolution during the cyclic voltammetry. Using low pH electrolyte led to hydrogen evolution before metal deposition. All solutions are freshly prepared with reagents from MERCK dissolved in bidistilled water, at 20 °C. The solutions were thoroughly deoxygenated by purging the cell with ultrapure nitrogen flow.

The electrochemical measurements were performed in a conventional three electrodes cell, using a potentiostat–galvanostat model 273A EG&G PAR. Cyclic voltammetry experiments were carried out at 20 mV/s, scanning initially towards negative potentials (−1 V). Chronoamperometric experiments were performed from an initial potential at which no process occurred to a potential at which reduction occurred. Three constant potentials were applied between the working electrode and the auxiliary electrode: −0.95, −1.0 and −1.1 V versus SCE. Surface morphologies of thick deposits were investigated ex situ by atomic force microscopy (AFM). Table 1 gives the plating solution compositions investigated.

Table 1
Electrolyte compositions

Deposit	$CoSO_4$ (mM)	$CoCl_2$ (mM)	$FeSO_4$ (mM)	H_3BO_3 (mM)	Na_2SO_4 (M)
Co	100	10		500	1
CoFe (1/1)	100	10	100	500	1
CoFe (10/1)	100	10	10	500	1

3. Results and discussion

3.1. Electrochemical study

Fig. 1 shows typical cyclic voltammogram obtained for the Pt/Si(1 0 0) electrode in 100 mM $CoSO_4$, 10 mM $CoCl_2$ and 1 M Na_2SO_4 with 500 mM H_3BO_3, at pH 3.8. The scanning rate was 20 mV/s. The curve shows the presence of cathodic and anodic peaks associated to a deposition and dissolution of Co. In the potential range were reduction of Co occurs, hydrogen evolution is also present. On the other hand cobalt deposition began around −0.8 V, when the scan was reversed the typically nucleation loop was detected, with a single oxidation peak centred at −0.29 V. This characteristic is consistent with nucleation followed by diffusion-limited growth [20]. The difference between the current onset in the forwards and reverse scan is related to the nucleation barrier.

In order to study the mechanism of the nucleation process at early stages of electrodeposition, and to determine the kinetics parameters, the transients current obtained from chronoamperometric experiments were analysed. Fig. 2 shows a series of deposition transients for Co at pH 3.8. All the transients exhibit an initial increase due to nucleation followed by a decrease in current associated with diffusion-limited growth. To study the mechanism of nucleation and growth, a theoretical model developed by Scharifker and Hills have been successfully applied to analyse the transient current deduced from

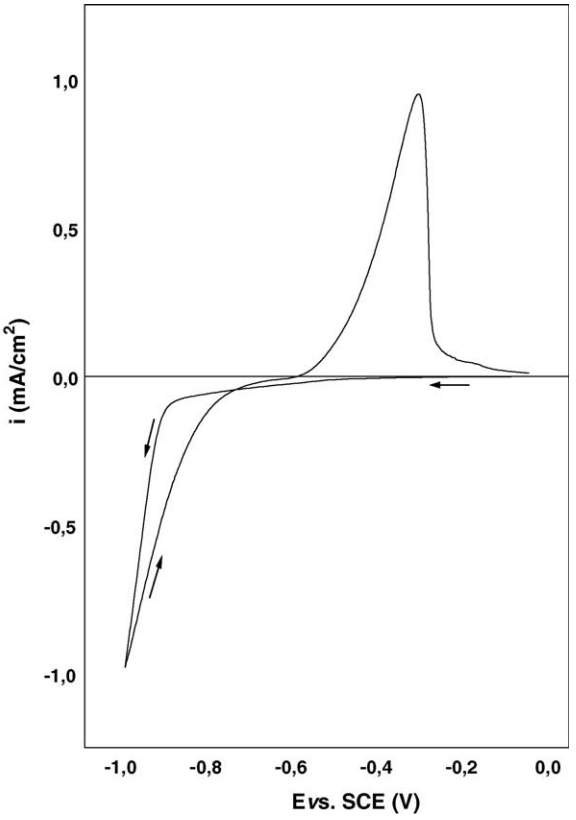

Fig. 1. Cyclic voltammograms for Co electrodeposition onto Pt/Si(1 0 0) from 100 mM $CoSO_4$, 10 mM $CoCl_2$ and 1 M Na_2SO_4 with 500 mM H_3BO_3 at pH 3.8. The scanning rate was 20 mV/s.

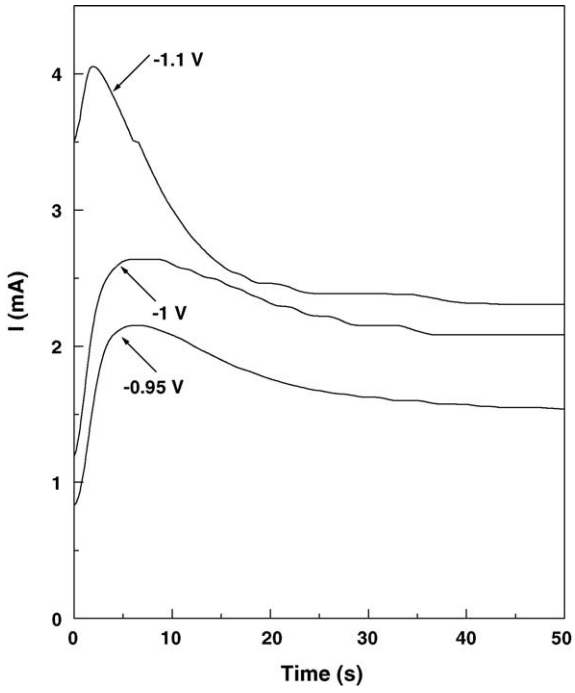

Fig. 2. Current transient for the electrodeposition of Co on Pt/Si(1 0 0) surface from the solution with pH 3.8 and at −0.95, −1 and −1.1 V vs. SCE, respectively.

chronoamperometric experiments [21,22]. According to theses authors the rate law for growth of 3D islands during electrochemical deposition is dependent on the mechanism of nucleation and growth. Models for electrochemical deposition onto foreign substrate usually assume that nucleation occurs at certain specific sites on the surface [23,24], and the nucleation mechanism is generally described in terms either of instantaneous or of progressive nucleation. If the rate of nucleation is rapid in comparison with the consequent rate of growth, subsequently nuclei are formed at all possible growth sites within very short times and nucleation is considered instantaneous. On the other hand, if the rate of nucleation is slow, subsequently nucleation will continue to take place at the surface while other clusters are growing and nucleation is considered progressive [25]. In order to distinguish between instantaneous and progressive nucleation process, experimental chronoamperometric data are used by representing in a non-dimensional plot $\frac{i^2}{i^2_{max}}$ versus $\frac{t}{t_{max}}$ and to compare these with the theoretical plots resulting from the following equations:

- For instantaneous nucleation followed by three-dimensional diffusion-limited growth is [21,22]:

$$\frac{i^2}{i^2_{max}} = 1.9542\left(\frac{t_{max}}{t}\right)\left[1-\exp\left(-1.2564\frac{t}{t_{max}}\right)\right]^2 \quad (1)$$

- and for progressive nucleation followed by three-dimensional diffusion-limited growth is [21,22]:

$$\frac{i^2}{i^2_{max}} = 1.2254\left(\frac{t_{max}}{t}\right)\left[1-\exp\left(-2.3367\frac{t^2}{t^2_{max}}\right)\right]^2 \quad (2)$$

Fig. 3 compares the experimental results obtained at −1 V versus SCE, with the two limiting cases of the theoretical three-dimensional nucleation growth models. It can be seen in this illustration that nucleation process of Co on Pt/Si(1 0 0) surfaces was classified as an instantaneous nucleation with diffusion controlled growth in accordance with those obtained through analysis of Fig. 2. These results suggest that, at deposition cathodic potentials related to −1 V, the nucleation sites become saturated after short times in comparison with the transient peak. This behaviour is in good agreement with morphological observations.

Verification of the mechanism of nucleation and growth can be obtained through determination of the diffusion coefficient D, and comparison with known values. The diffusion coefficient of the metal ion is calculated by means value of the product $i^2_{max}t_{max}$ [21,22].

For instantaneous nucleation:

$$D = \frac{i^2_{max}t_{max}}{0.1629(zFc)^2} \quad (3)$$

and for progressive nucleation:

$$D = \frac{i^2_{max}t_{max}}{0.2598(zFc)^2} \quad (4)$$

For instantaneous nucleation the nucleus density can be determined by equation:

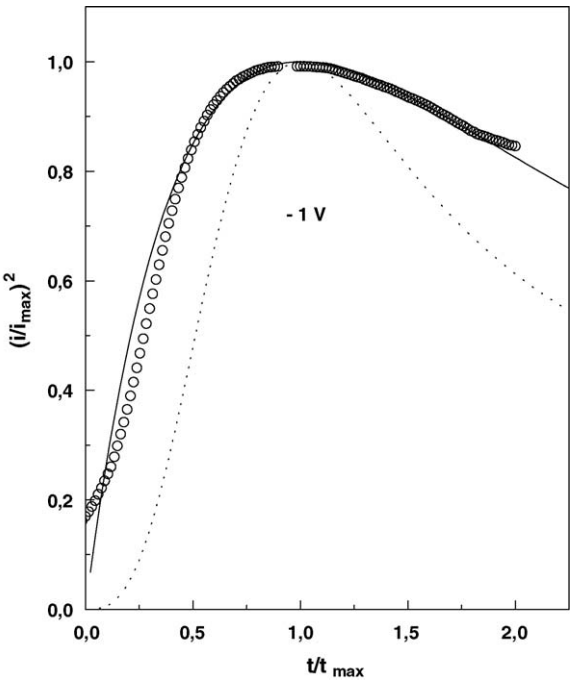

Fig. 3. Current transient for deposition of Co on Pt/Si(1 0 0), at −1 V vs. SCE plotted in dimensionless form. The dashed and full lines represent the theoretical curves for progressive and instantaneous limiting cases, respectively.

$$N_\infty = 0.065\left(\frac{8\pi cM}{\rho}\right)^{-1/2}\left(\frac{zFc}{i_{max}t_{max}}\right)^2 \quad (5)$$

and for progressive nucleation, the nucleation rate AN_∞ is given by the following equation:

$$AN_\infty = 0.2898\left(\frac{8\pi cM}{\rho}\right)^{-1/2}\left(\frac{zFc}{i_{max}^2 t_{max}^3}\right)^2 \quad (6)$$

where c is the concentration of metal ions in the bulk solution, M the molar weight of the deposit, z the valence of the metal ion, F the Faraday's constant and ρ is the density of the film.

Based on chronoamperometric experiments data and the mechanism of nucleation, the characteristic parameter such as nuclei density N_∞ is determined by Eq. (5). The diffusion coefficients (D) employed was determined from mean value of the quantify $i_{max}^2 t_{max}$ which is 5.77×10^{-6} cm^2 s^{-1} for Co. The values thus obtained appeared in Table 2.

Then according to theses values it can be deduced that increased E leads to less nuclei density (N_∞). This is possible when the saturation state is reached.

For CoFe alloys deposition through solutions with various compositions of Co and Fe were investigated. The ratio molar Co/Fe used in this study were (1/1) and (10/1). The voltammetric response was shown in Fig. 4. This experiment was carried out with the same conditions used in the electrodeposition of individual Co. The characteristic loop of nucleation is clearly observed in this curve. The anodic peak appears at this case at −0.28 V. This difference in comparison with the anodic peak of individual Co is due probably to the co-deposition phenomena. The chronoamperometric responses obtained on Pt/Si(1 0 0) surfaces from solution containing the molar ratio (1/1) and (10/1) are presented in Fig. 5(a) and (b), respectively. The amperometric experiments were carried at −0.95, −1.0 and −1.1 V versus SCE. The current transients presented similar behaviours, currents increase to a maximum and decrease gradually with time. The rising of these currents is corresponding to the growth of a new phase. Fig. 6(a) and (b) show non-dimensional plots data for CoFe (1/1) and CoFe (10/1) alloys, respectively, the applied potential was fixed at −1.0 V versus SCE. The analysis of the transients current was made by using Scharifker and Hills model as described in Eqs. (3) and (4). The results indicated that experimental transients for CoFe (10/1) alloy electrocrystallization closely follow the instantaneous theoretical model, and for CoFe (1/1) alloy the nucleation was in agreement with the progressive model. According to theses results it can be seen that the

Table 2
Analysis of the current maximum for Co deposition

$-E_{step}$ (V)	t_{max} (s)	$-i_{max}$ (mA/cm^2)	N_∞ ($\times 10^{-5}$ cm^{-2} s^{-1})
0.95	5.9	7.16	1.04
1.0	5.3	8.66	0.90
1.1	4.8	13.22	0.46

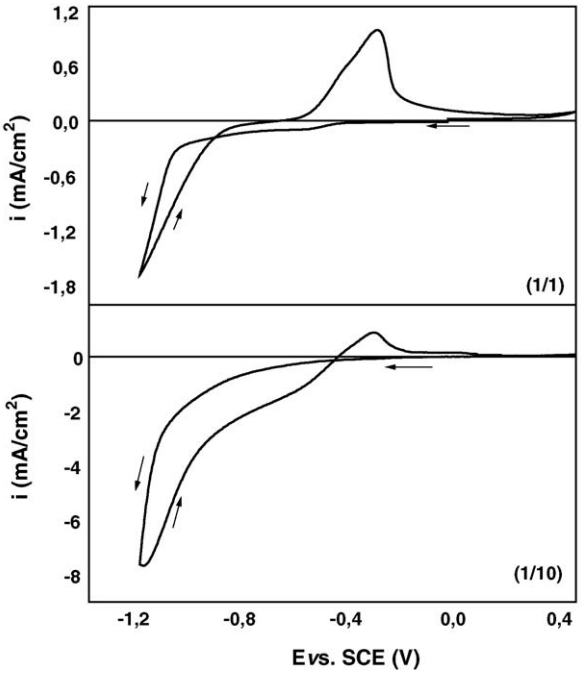

Fig. 4. Cyclic voltammograms for CoFe electrodeposition onto Pt/Si(1 0 0) from 100 mM $CoSO_4$ + 10 mM $CoCl_2$ + 100 mM $FeSO_4$ (ratio 1/1), 100 mM $CoSO_4$ + 10 mM $CoCl_2$ + 10 mM $FeSO_4$ (ratio 10/1), in 1 M Na_2SO_4 and 500 mM H_3BO_3 solutions at pH 3.8. The scanning rate was 20 mV/s.

composition of the electrolyte influence greatly the type of nucleation. Thus the nucleation mechanism of alloys obtained with lower rate of Fe was the same mechanism observed in individual metal deposition Co, conversely, if the rate of Fe was present in a considerable amount, the mechanism of nucleation changed and was consistent with the progressive nucleation. A progressive nucleation mechanism followed by 3D growth is established for CoFe electrodeposited at pH 2 in chloride solution [17]. In mixed chloride sulfate solution, no literature data were found for CoFe electrodeposition. Also, it is not possible to use the Scharifker and Hills model to estimate the nuclei density of alloys or to evaluate kinetics parameters, and nothing has been found in the literature.

3.2. Ex situ AFM studies

AFM surface topography gives further support to theses results of nucleation mechanism. Fig. 7 shows typical ex situ 3D AFM images of (a) Pt/Si(1 0 0) substrates, (b) Co films electrodeposited at −1 V for 100 s and (c) CoFe (10/1) alloys electrodeposited at −1 V for 300 s. The films have uniform, compact and granular structure. Also, the figures reveal that the Co and CoFe cover all the substrate and the grain size varies during the surface of the film. The Co and CoFe films were also analysed by energy-dispersive spectroscopy (EDS) and no trace of oxide or other contamination was found near the detection limit. From the AFM measurements the root mean square (RMS) surface roughness was calculated over the 4 μm × 4 μm area for Pt/Si(1 0 0) substrates, Co films and CoFe (10/1) alloy. The RMS parameter is equal to 10.9, 8.95

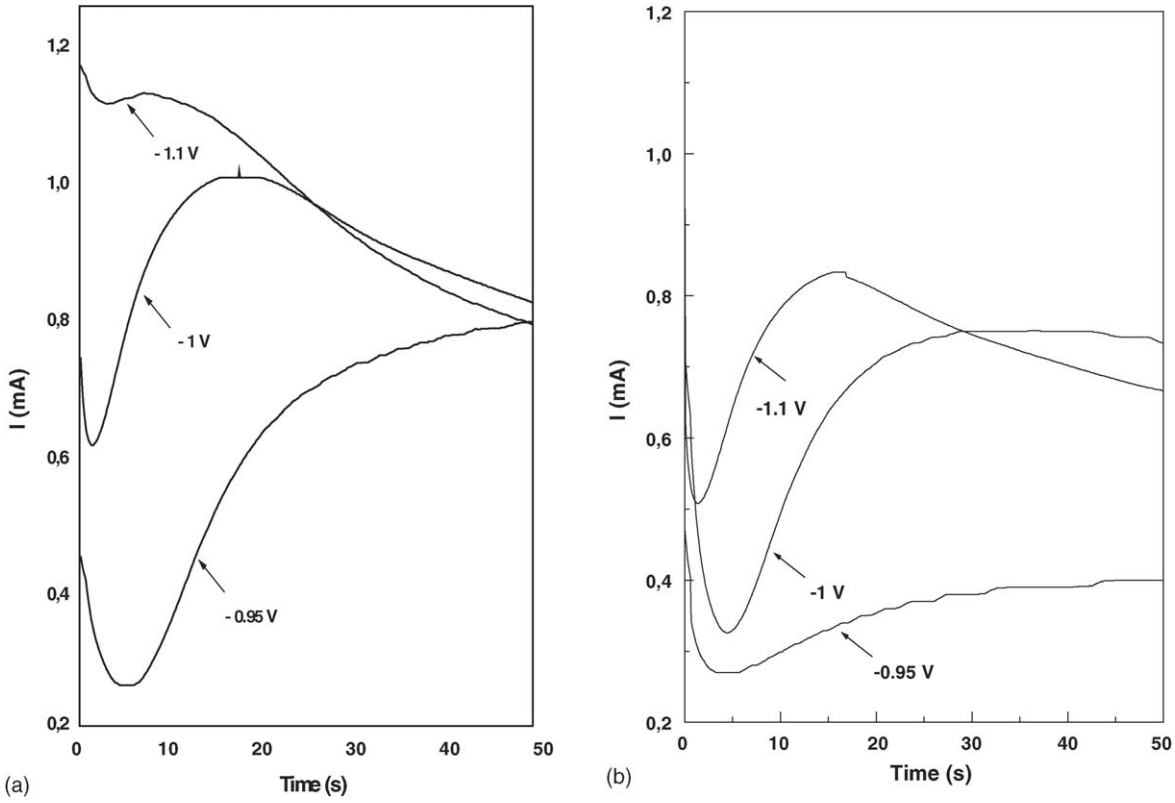

Fig. 5. (a) Current transient for the electrodeposition of CoFe (1/1) alloy on Pt/Si(1 0 0) surface from the solution with pH 3.8 and at −0.95, −1 and −1.1 V vs. SCE, respectively. (b) Current transient for the electrodeposition of CoFe (10/1) alloy on Pt/Si(1 0 0) surface from the solution with pH 3.8 and at −0.95, −1 and −1.1 V vs. SCE, respectively.

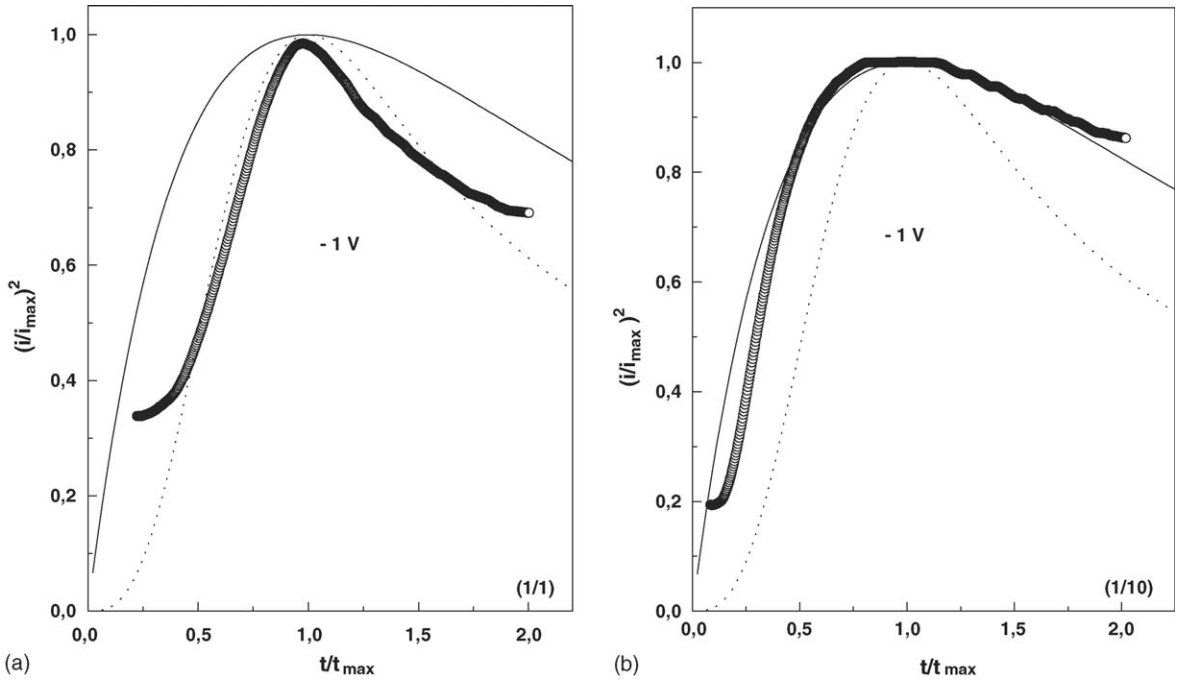

Fig. 6. (a) Current transient for deposition of CoFe (1/1) alloy at −1 V vs. SCE plotted in dimensionless form. The dashed and full lines represent the theoretical curves for progressive and instantaneous limiting cases, respectively. (b) Current transient for deposition of CoFe (10/1) alloy at −1 V vs. SCE plotted in dimensionless form. The dashed and full lines represent the theoretical curves for progressive and instantaneous limiting cases, respectively.

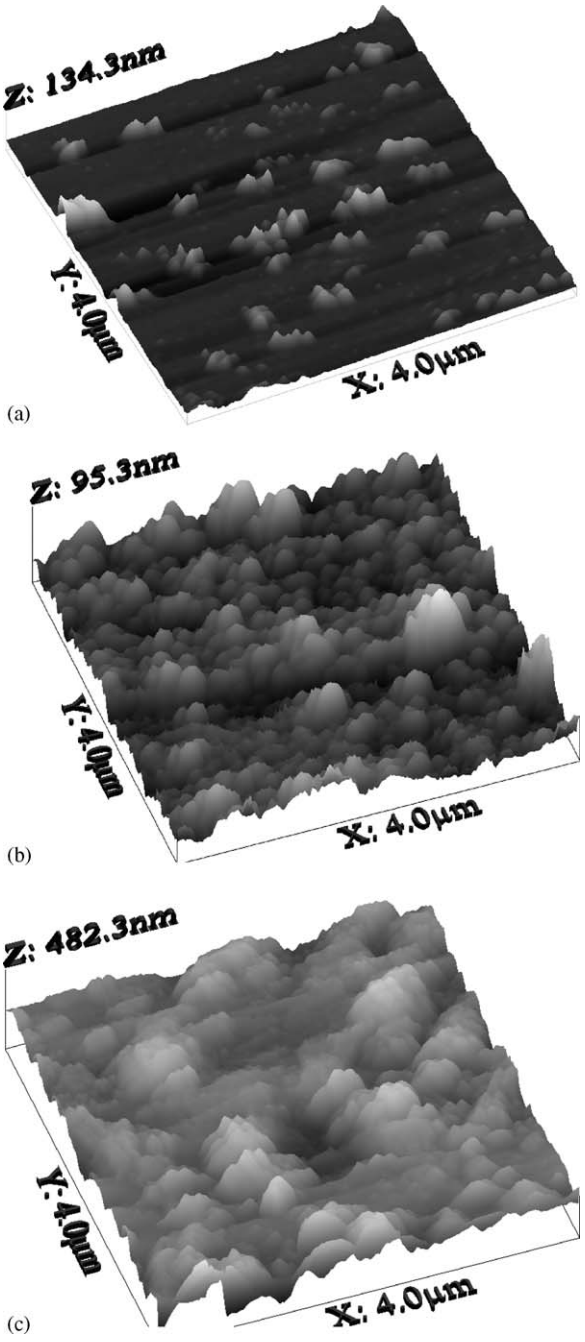

Fig. 7. 3D AFM images (4 μm × 4 μm) of the surface topography of (a) Pt/Si(1 0 0) substrates, (b) Co films at −1 V after deposition for 100 s and (c) CoFe layer at −1 V after deposition for 300 s.

and 45.14 nm for Pt/Si(1 0 0), Co and CoFe films, respectively. It is difficult to compare this result with the literature data because RMS parameter strongly depends on the scan length and the films thickness.

4. Conclusion

In this study we have presented a nucleation study of the electrodeposition of Co and CoFe alloys on Pt/Si(1 0 0) surface in mixed chloride sulfate solutions. The obtained electrodeposited samples take place through 3D island nucleation process with controlled growth and show an instantaneous nucleation mechanism for Co layers and CoFe (10/1) alloys. For CoFe (1/1) alloy the nucleation was in agreement with the progressive mechanism. It is clear; the influence of the co-deposition phenomena and the composition chemistry is in the mode of nucleation and growth.

Acknowledgements

This work was supported financially by the collaborative French-Algerian program CMEP No. 04 MDU 608 under the supervision of EGIDE, between the University Louis Pasteur of Strasbourg, France and the University Ferhat Abbas of Sétif, Algeria.

References

[1] P.L. Cavallotti, N. Lecis, H. Fauser, A. Zielonka, J.P. Celis, G. Wouters, J. Machado da Silva, J.M. Brochado Oliveira, M.A. Sa, Surf. Coat. Technol. 105 (1998) 232.
[2] J.P. Celis, P. Cavallotti, J. Machado Da Silva, A. Zielonka, Trans. Inst. Met. Finish. 76 (1998) 163.
[3] T. Osaka, Electrochim. Acta 45 (2000) 3311.
[4] J.L. Bubendorff, E. Beaurepaire, C. Mény, P. Panissod, J.P. Bucher, Phys. Rev. B 56 (1997) 7120R.
[5] A.N. Correia, S.A.S. Machado, L.A. Avaca, J. Electroanal. Chem. 488 (2000) 110.
[6] E. Goméz, M. Marin, F. Sanz, E. Valles, J. Electroanal. Chem. 422 (1997) 139.
[7] A.B. Soto, E.M. Arce, M.P. Pardave, I. Gonzalez, Electrochim. Acta 41 (1996) 2647.
[8] M.P. Pardave, I. Gonzalez, A.B. Soto, E.M. Arce, J. Electroanal. Chem. 443 (1998) 125.
[9] R. Bertazzoli, A.D.F.B. Sousa, J. Braz. Chem. Soc. 8 (1997) 357.
[10] A. Azizi, A. Sahari, M.L. Felloussia, G. Schmerber, C. Mény, A. Dinia, Appl. Surf. Sci. 228 (2004) 320.
[11] J.L. Bubendorff, C. Meny, E. Beaurepaire, P. Panissod, J.P. Bucher, Eur. Phys. J. B 17 (2000) 635.
[12] S. Vilain, J. Ebothe, Mater. Sci. Eng. C 15 (2001) 199.
[13] L. Ricq, F. Lallemand, M.P. Gigandet, J. Pagetti, Surf. Coat. Technol. 138 (2001) 278.
[14] K.Y. Sasaki, J.B. Talbot, J. Electrochem. Soc. 145 (1998) 981.
[15] S.I. Berezina, L.G. Sharapova, V.G. Shtyrlin, Y.P. Khodyrev, Prot. Met. 30 (1994) 154.
[16] E.L. Abd, S.S. Rehim, K. Khaled, A.M.S. Abulkibash, M. Emad, Trans. Inst. Met. Finish. 78 (2000) 41.
[17] F.R. Bento, L.H. Mascaro, J. Braz. Chem. Soc. 13 (2002) 502.
[18] R. Bertazzoli, D. Pletcher, Electrochim. Acta 38 (1993) 671.
[19] A. Brenner, Electrodeposition of Alloys, vols. 1 and 2, Academic Press, New York, 1963.
[20] R. Sonnenfeld, J. Schneier, P.K. Hansma, in: R.E. White, J.O'M. Bockris, B.E. Conway (Eds.), Modern Aspects of Electrochemistry, vol. 21, Plenium, New York, 1990.
[21] B.R. Scharifker, G.J. Hills, Electrochim. Acta 28 (1983) 879.
[22] E. Bosco, S.K. Rangarajan, J. Electroanal. Chem. 134 (1982) 213.
[23] E.B. Budevski, in: E. Conway, et al. (Eds.), Comprehensive Treatise of Electrochemistry, vol. 7, Plenum, New York, 1983, p. 399.
[24] L.T. Romankiw, T.A. Palumbo, in: L.T. Romankiw, D.R. Turner (Eds.), Electrodeposition Technology, Theory and Practice, Electrochemical Society, Pennington, NJ, 1988, p. 13.
[25] G. Oskam, J.G. Long, A. Natarajan, P.C. Searson, J. Phys. D: Appl. Phys. 31 (1998) 1927.